I&EC research
Industrial & Engineering Chemistry Research

Article

pubs.acs.org/IECR

Portland Cement Paste Modified by TiO_2 Nanoparticles: A Microstructure Perspective

Decheng Feng,[†] Ning Xie,*[,†,‡,§] Chunwei Gong,[†] Zhen Leng,[⊥] Huigang Xiao,[‡] Hui Li,[‡] and Xianming Shi*[,†,§]

[†]School of Transportation Science and Engineering and [‡]School of Civil Engineering, Harbin Institute of Technology, Harbin 150001, China

[§]Corrosion and Sustainable Infrastructure Laboratory, Western Transportation Institute and Civil Engineering Department, P.O. Box 174250, College of Engineering, Montana State University, Bozeman, Montana 59717-4250, United States

[⊥]Department of Civil and Environmental Engineering, Hong Kong Polytechnic University, 11 Yuk Choi Road, Hung Hom, Hong Kong

ABSTRACT: Nanomodified Portland cement paste with a water/cement ratio of 0.4 was prepared with the addition of TiO_2 nanoparticles at 0.1, 0.5, 1.0, and 1.5% by mass of cement. The flexural strengths of the prepared cement-based composites were tested, and the fracture surfaces were observed by scanning electron microscopy (SEM). The flexural strength of the nanomodified TiO_2 Portland cement paste reached the highest value with a dosage of 1.0 mass %. The SEM observation shows that admixing of the TiO_2 nanoparticles largely decreased the quantity of internal microcracks in the cement paste. A new type of needle-shaped hydration product was observed, and its potential growth mechanism was proposed. Atomic force microscopy was introduced to observe the microstructure of nanomodified Portland cement paste, and the results show that the nanoroughness of the hardened cement pastes with admixed TiO_2 nanoparticles was much lower than that without the TiO_2 nanoparticle addition. Coupled with X-ray diffraction data, the morphological information obtained at the micrometer and nanometer scales shed light on the role of TiO_2 nanoparticles in the cement-based composite.

1. INTRODUCTION

Portland cement is a commonly used binder material to form the heterogeneous mortar or concrete matrix, and the durability of concrete structures and components in service environments is of great interest to practicing engineers and researchers.[1−5] In this context, many approaches have been investigated to improve the durability properties of concrete, with a focus on modification of the binder.[6−9] As a promising emerging technology in construction, nanotechnology has been applied in the production of concrete and proven to enhance the mechanical properties (e.g., compressive strength, ductility, impact resistance) and reduce shrinkage and permeability, all of which contribute to extension of the concrete's service life.[10−13]

A wide variety of nanosized materials, such as nanoclays, Fe_2O_3 and SiO_2 nanoparticles, carbon nanotubes, and TiO_2 nanoparticles, have been used to reduce the permeability or improve the mechanical properties of concrete, thanks to the decreasing production cost of nanomaterials and the increasing need for multifunctional materials over the last 2 decades. He and Shi[14] summarized the possible mechanisms responsible for the beneficial effect of nanomaterials on the impermeability of mortar and concrete. These may include 1) working as nanosized fillers and leading to a denser and less permeable microstructure, (2) acting as a "nucleus" to guide the formation and growth of cement hydration products, and (3) promoting the formation of high-density C−S−H structures via parallel packing. In addition, SiO_2 nanoparticles and nanomontmorillonites are used, and a pozzolanic reaction may occur between the Portland cement paste and SiO_2 in nanomaterials.[14] The nanosheets of montmorillonites distributed in the mortar or concrete matrix may also introduce microstructural regularity and serve as a dense barrier and "fiber reinforcement". Li et al.[15,16] claim that the nanoparticles can act as nuclei during the hydration process, and Shah et al. further suggested that they can fill the voids in the cement matrix and induce the formation of better C−S−H.[17] Previous studies also demonstrated that nanoparticles can strengthen the interfacial transition zone between the cement paste and aggregate, thus improving the strength and impermeability of concrete.[18] Makar and Chan[19] reported single-walled carbon nanotubes to accelerate the hydration reaction of the tricalcium silicate (C_3S) in ordinary Portland cement and affect the morphology and location of both the initial tricalcium aluminate (C_3A) and the C_3S hydration products. Vera-Agullo et al.[20] reported that with proper dispersion the carbon nanofilaments (either multiwalled nanotubes or nanofibers) accelerated the cement hydration process and so did the nanosilica and nanoclays.

Titanium exists in minerals, mostly rutile and ilmenite, which are widely distributed in the earth's crust and lithosphere. Titanium is ubiquitous in the natural environment, such as rocks, water bodies, and soils. TiO_2 nanoparticles have exhibited many magnificent advantages in daily products, including white paint, plastics, papers, inks, foods, medicines, makeups, and toothpastes. They have also shown desirable properties for such applications as environmental preservation

Received: April 11, 2013
Revised: July 16, 2013
Accepted: July 22, 2013
Published: July 22, 2013

dx.doi.org/10.1021/ie4011595 | *Ind. Eng. Chem. Res.* 2013, 52, 11575−11582

and energy harvesting, including photocatalytic water splitting, heterogeneous photocatalysis, charge transfer, Gratzel cells, sensitized solar cells, organic photovoltaic cells, quantum dots, nanorods, nanotubes, photocurrent generation, and electrodes.[21]

In recent years, some researchers fabricated cement-based concrete or asphalt concrete incorporating TiO_2 nanoparticles to improve their durability or endow them with certain desirable functionality.[22−24] Nanotechnology has demonstrated its substantial benefits in empowering the development of concrete with enhanced durability and mechanical properties.[25−27] Yet, the mechanisms of concrete nanomodification, particularly by TiO_2 nanoparticles, remain unclear. One hypothesis to test is that the admixing of TiO_2 nanoparticles into cement not only leads to denser hardened cement paste but also alters the morphology and chemical compositions of cement hydration products.

The early-age performance of cement-based materials modified by TiO_2 nanoparticles has been studied by some researchers. The admixing of TiO_2 nanoparticles into cement-based materials was found to increase their heat of hydration and accelerate their hydration via heterogeneous nucleation.[28] The early-age mechanical properties were reported to increase with the addition of TiO_2 nanoparticles. The later-age mechanical properties, however, decreased sharply as the dosage of TiO_2 nanoparticles increased from 5% to 10% by weight of cement.[29] This is attributable to the increased agglomeration of nanoparticles at higher dosage.

The effect of TiO_2 nanoparticles on the early-age hydration kinetics of tricalcium silicate (C_3S) was investigated by Lee and Kurtis[30] via the Avrami model[31−33] shown as

$$X = 1 - \exp[-(k_{avr}t)^n] \tag{1}$$

where X is the transformed volume fraction as a function of time and k_{avr} is the effective rate constant as a function of the constant linear growth rate. If eq 1 is differentiated with respect to time, the hydration rate can be obtained as

$$R = Ank_{avr}{}^n(t - t_0)^{n-1} \exp\{-[k_{avr}(t - t_0)^n]\} \tag{2}$$

where R is the hydration rate, A is a normalization constant to match the isothermal calorimetry data, and t_0 is the time delay between the time of mixing and the start of nucleation and growth kinetics.

Recently, the boundary nucleation model was modified by Thomas[34] to describe the hydration kinetics of C_3S, shown as

$$X = 1 - \exp\{-2O_v^B \int_0^{G_T} [1 - \exp(-Y^e)]\, dy\} \tag{3}$$

where

$$Y^e = \frac{\pi I_B}{3} G^2 t^3 \left[1 - \frac{3y^2}{G^2t^2} + \frac{2y^3}{G^3t^3}\right] \quad \text{if } t > \frac{y}{G}$$

$$Y^e = 0 \quad \text{if } t < \frac{y}{G} \tag{4}$$

Here, y and Y^e are temporary variables that disappear after integration, X depends on three well-defined physical parameters: G, the linear growth rate of the transformed phase; I_B, the nucleation rate per unit area of the untransformed boundary; and O_v^B, the boundary area per unit volume. The author claimed that the addition of TiO_2 nanoparticles increased the peak reaction rate and the degree of early-age hydration. It was also claimed that the hydration products formed on or near the surfaces of TiO_2 nanoparticles and the C_3S surface as well. These results demonstrate that the addition of TiO_2 nanoparticles accelerates the early-age hydration by providing additional nucleation sites, laying the groundwork for the fabrication of cement-based materials with nanoparticles incorporated.

Calcium silicate hydrate (C−S−H), as the main binding phase in concrete, has been extensively studied. It was claimed that C−S−H in a hardened paste of C_3S or Portland cements generally has an average Ca/Si ratio of about 1.75 and ranges from about 1.2 to 2.1 in any given paste.[35] There are some models that demonstrated the nanostructure of C−S−H,[36] mainly falling into two types. One type of C−S−H is where the silicate anions are entirely monomeric, and the other one is where a linear silicate chain is present in 1.4 nm tobermorite (and a number of other minerals), i.e., dreierkette-based models.[37] Yet another solid C−S−H model was developed by using the H_2O/D_2O small-angle neutron scattering contrast variation method. In this model, the nanoscale $Ca(OH)_2$ phase was quantified and the solid C−S−H formula, $(CaO)_x(SiO_2)$-$(H_2O)_y$, was determined in terms of x and y, together with its mass density.[38] Bernal[39] believed that most of the silica in the hydration products in cement paste can be divided into two types of hydrated calcium silicates, demonstrated as $C_2SH(II)$ and CSH(I). It was claimed that both of these phases included the monomeric silicate anion $[SiO_2(OH)_2]_2^-$ with the general formula given as $Ca[SiO_2(OH)_2][Ca(OH)_2]_xH_2O_y$, where x would be 1 for $C_2SH(II)$ and between 0 and 0.5 for CSH(I).

In the past decade, the rapid progress and improved availability of advanced nanomaterials and characterization techniques have led to numerous engineering and mechanistic studies of nanotechnology for cementitious materials.[40−42] Recently, many technologies such as nuclear magnetic resonance,[43] small-angle X-ray scattering,[44] small-angle neutron scattering,[45] and the pair distribution function approach have been utilized to elucidate the microstructure of the paste clinker at nanoscale.[46] Scanning electron microscopy with energy-dispersive spectrometry (SEM/EDS)[47] and transmission electron microscopy (TEM)[48] have been used for observing the microstructure and morphology and for analyzing the chemical composition of cement-based materials. Atomic force microscopy (AFM) has been used for observing the morphology at nanoscale and for evaluating nanoscale mechanical properties.[49] Furthermore, differential scanning calorimetry[50] and X-ray diffraction (XRD)[51] have been used to analyze the hydration products and crystalline structures of Portland cement paste, respectively.

The microstructures of Portland cement paste incorporating nanosized SiO_2, Fe_2O_3, and carbon nanotubes have been reported.[16,52,53] However, to the best of our knowledge, the microstructure of the hardened Portland cement paste incorporating nanosized TiO_2 has not yet been reported. This work aims to address this knowledge gap by shedding light on the microstructure of nanomodified TiO_2 cement paste, particularly at the nanometer and submicrometer scales.

2. EXPERIMENTAL SECTION

The cement-based materials were made from normal Portland cement pastes (no. 42.5) purchased from Yatai Corp., and the TiO_2 nanoparticles were offered by Kaier Corp., China. The chemical compositions of the cement and TiO_2 are listed in Table 1. The water/cement ratio was 0.4 for all samples. No

dx.doi.org/10.1021/ie4011595 | Ind. Eng. Chem. Res. 2013, 52, 11575−11582

Table 1. Chemical Composition (%) of the Cement and TiO_2 Nanoparticles

	cement	TiO_2
SiO_2	20.4	
Al_2O_3	3.7	
Fe_2O_3	3.4	
SO_3	2.6	
CaO	63.3	
Na_2O	0.1	
K_2O	0.4	
MgO	3.2	
TiO_2		>99.5
loss of ignition	2.7	

admixtures or additives other than TiO_2 nanoparticles were added into the cement paste. The dosages of TiO_2 nanoparticles were 0.1%, 0.5%, 1.0%, and 1.5%, respectively, by mass of cement.

Before mixing the TiO_2 nanoparticles and cement, the TiO_2 nanoparticles were soaked in water and ultrasonically vibrated for 30 min to achieve good distribution. This was followed by another 3 min of mixing of the water with the cement under a stirring rate of 800 rph. A 1-L beaker was used for the stirring process. After stirring, the mixture was poured into a plastic Petri dish with dimensions of ⌀ 50 mm × 15 mm. The specimens were demolded after 24 h and cured at room temperature for 28 days under a relative humidity of 95%. After curing, the samples were mechanically cut for the flexural strength test with a size of 3 × 4 × 40 mm^3. The flexural strength test followed the ASTM D790 method, and the span of the two end points was 33 mm and the loading speed was 0.5 mm/min.

The morphology of the TiO_2 nanoparticles was observed by TEM and selected area electron diffraction (SAED), which were performed on a Phillips Tecnai 20 microscope with an accelerating voltage of 200 kV. Figure 1 shows the TEM morphology and the SAED pattern of the TiO_2 nanoparticles,

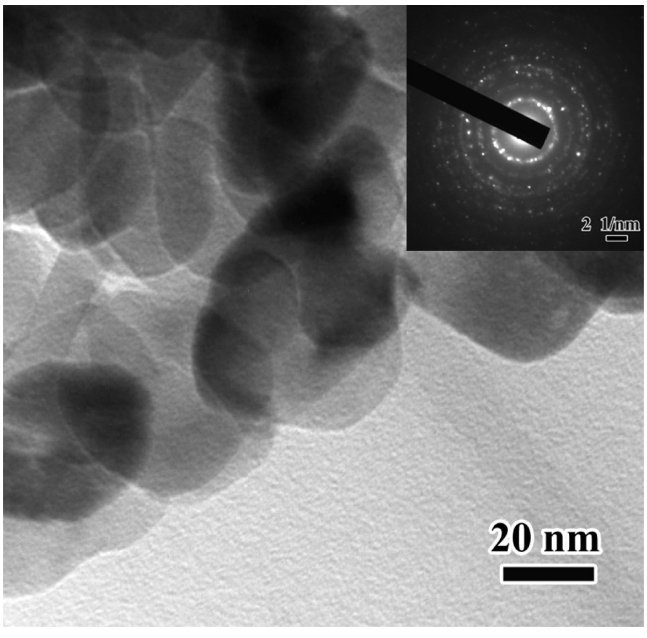

Figure 1. TEM morphology and its SAED of the TiO_2 nanoparticles.

which reveals that the TiO_2 nanoparticles are equiaxed nanocrystals with average particle sizes of about 20−50 nm.

The morphology of the fracture surface of the hardened cement samples was observed by SEM coupled with EDS, performed on a FEI-Quanta 200F scanning electron microscope. XRD of the samples was obtained on a Rigaku D/max-rA X-ray diffractometer with Cu Kα radiation (λ = 1.5406 Å).

The mechanically obtained AFM data were utilized to visually illustrate the microstructure and to generate roughness and other morphological information about the paste. For AFM imaging in this study, the cement paste surface examined was the as-fabricated bottom surface without polishing so as to avoid any potential disturbance of the surface condition by polishing. The AFM height and deflection images were obtained in contact mode, where the tip of the atomic force microscope stayed in contact with the sample while it was moved across. Roughness measurements were made by performing power spectral density measurements, as detailed elsewhere.[34] The phase images were obtained under the tapping mode.

3. RESULTS AND DISCUSSION

Figure 2 presents the 28-day three-point flexural strength as a function of the TiO_2 nanoparticle dosage by mass of cement,

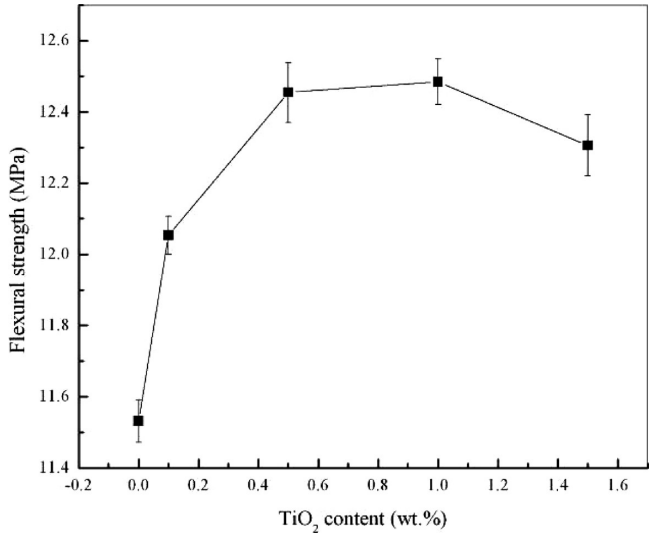

Figure 2. Three-point flexural strength as a function of the TiO_2 nanoparticle dosage in the cement paste.

when the water-to-cement mass ratio is fixed at 0.4. Each point shown in Figure 2 shows the average value and the standard deviation of flexural strength values from five specimens. Figure 2 reveals that admixing a small dosage (0.1 mass %) of the TiO_2 nanoparticles into the cement can increase its flexural strength by 4.5% (from 11.53 to 12.05 MPa). However, the benefits diminished with a further increase in the dosage of the TiO_2 nanoparticles. The flexural strength of cement paste reached the peak value 12.48 MPa, with 1.0 mass % of the TiO_2 nanoparticles admixed. As discussed later, the improvement of the flexural strength by nanomodification may be attributed to several mechanisms. First, the TiO_2 nanoparticles acted as nuclei to form needle-shaped hydration products, which can bridge the microcracks and fill in the micropores. Second, the TiO_2 nanoparticles altered their adjacent environment for cement hydration reaction and facilitated the formation of high-

dx.doi.org/10.1021/ie4011595 | Ind. Eng. Chem. Res. 2013, 52, 11575−11582

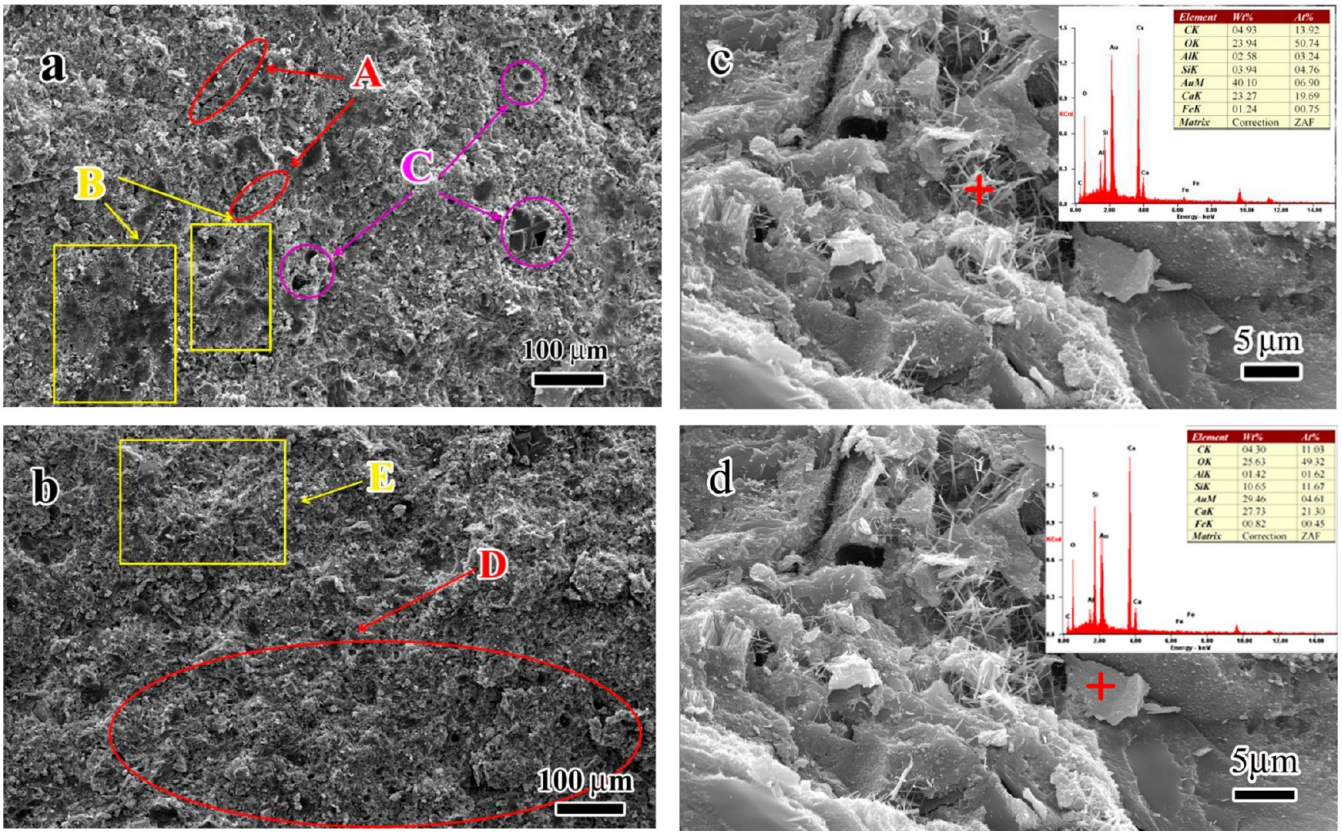

Figure 3. SEM morphology of the fracture surfaces: (a) low magnification of regular cement paste; (b) low magnification of cement paste modified by TiO_2 nanoparticles; (c and d) high magnification of cement paste modified by TiO_2 nanoparticles (inset: EDS data).

density C−S−H over low-density C−S−H. Finally, the TiO_2 nanoparticles led to more evenly distributed hydration phases, which feature the higher fracture energy inherent in the cement paste. Note that fully achieving the potential of nano-modification hinges on the proper dispersion of the nanoparticles in the heterogeneous matrix of a cement-based composite. The agglomeration of nanoparticles may at least partly explain the trends observed in Figure 2, especially the decrease of the flexural strength with the increase of TiO_2 nanoparticles from 1.0 to 1.5 mass %.

Figure 3 presents the low- and high-magnification SEM images of the fracture surfaces of the hardened Portland cement paste with or without the addition of TiO_2 nanoparticles (at 1.0 mass %). In the low-magnification mode, as shown in Figure 3a, some microcracks perpendicular to the crack surface of the sample can be observed (area A) along with some flat areas exhibiting surfaces of microcracks parallel to the crack surface of the sample (area B) and some areas with clear internal defects and micropores (area C). As shown in Figure 3b, with the addition of TiO_2 nanoparticles, the hydration products were distributed more evenly in the cement-based composite (area D), and the density and size of the microcracks and micropores were greatly decreased. Meanwhile, some nanosized needle-shaped hydration products can be observed (area E). Parts c and d of Figure 3 show the high-magnification image and EDS results of the needle-shaped hydration products in the area E in Figure 3b. As can be seen from the EDS results, the chemical composition of the needle-shaped hydration products differed from that of the other phase adjacent to it. Despite their comparable calcium contents, the former featured a Ca/Si ratio of 5:1 and an Al/Si ratio of 3:5, whereas the latter featured a Ca/Si ratio of 2:1 and an Al/Si ratio of 1:6. These aluminum-rich and silicon-deficient needle-shaped precipitates could be a new type of C−S−H, which needs to be further elucidated in future studies. Compared with the regular Portland cement hydrates, these precipitated nanosized needle-shaped products can fill the submicrometer pores and cracks in the paste more efficiently and reinforce the paste by bridging the cracks.

In the past decades, the fiber-reinforced composites have been extensively studied and the beneficial role of fibers in improving the toughness of the composite has been confirmed.[55,56] The needle-shaped hydration products observed in a nanomodified cement paste (Figure 3) will act as nanofibers to be pulled out of bent during propagation of cracks and bridge the cracks at the microscopic level. In other words, they are expected to help toughen the cement paste. These can be considered as in situ fiber reinforcement to feature higher bonding strength with the rest of the cement paste matrix, related to admixed fibers. Additional research is warranted to elucidate the quantity, dimensions, and mechanical properties of these needle-shaped hydration products and how they contribute to the macroscopic properties of the cement paste.

Figure 4 presents the AFM data of the regular cement paste and the cement paste modified with TiO_2 nanoparticles at 1.0 mass %, in a 1×1 μm^2 area. As can be seen in this figure, the regular cement paste and nanomodified TiO_2 cement paste feature a microstructure with distinct characteristics. While the microstructure of the regular concrete was very rough (Figure 4a), the nanomodified cement paste appeared to be much more flat (Figure 4b). It can be demonstrated from Figure 4c,d that

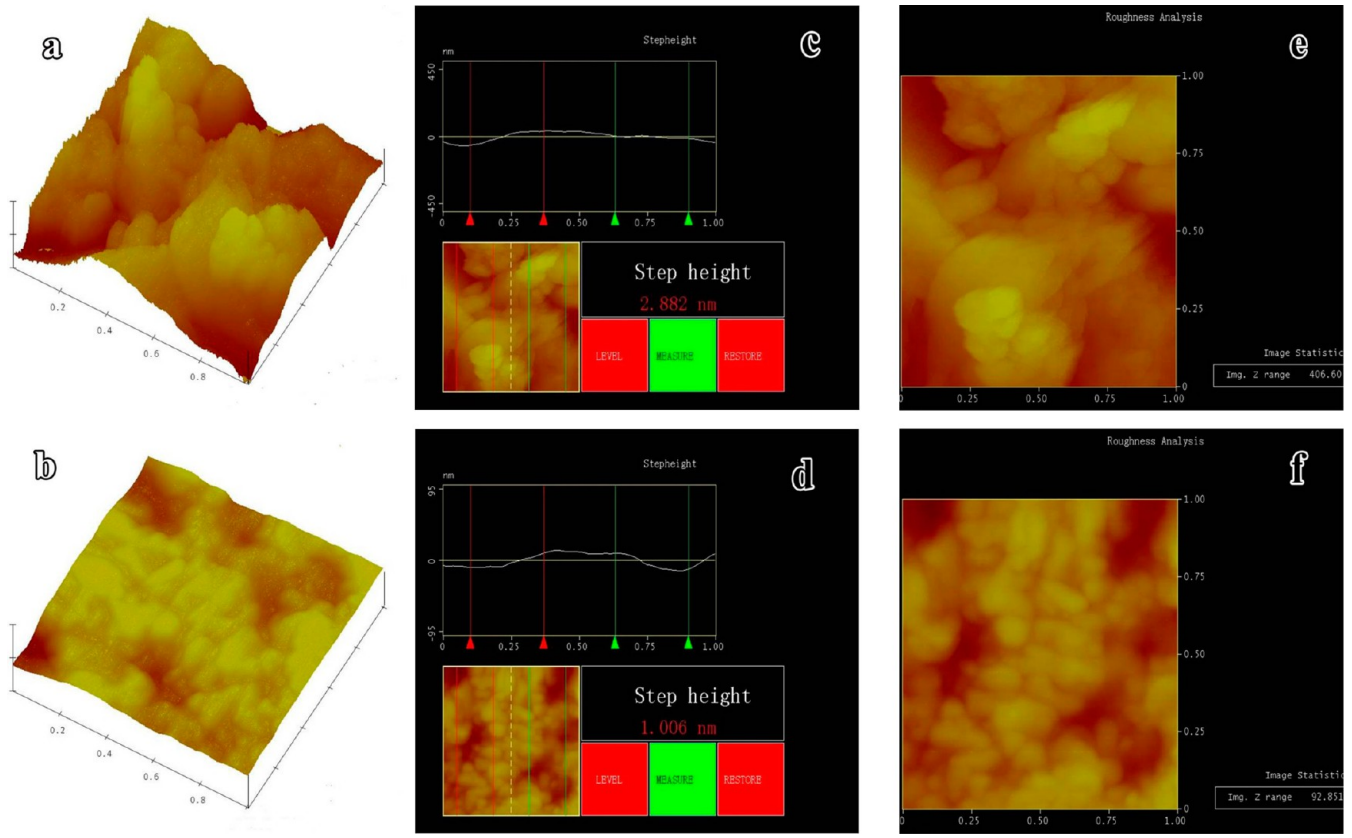

Figure 4. AFM observations of (a) height image of regular cement paste, (b) height image of cement paste modified by TiO_2 nanoparticles, (c) step height of regular cement paste, (d) step height of cement paste modified by TiO_2 nanoparticles, (e) roughness of regular cement paste, and (f) roughness of cement paste modified by TiO_2 nanoparticles in a 1×1 μm^2 area.

the step heights of the regular and nanomodified cement paste were 2.882 and 1.006 nm, respectively.

The roughness test enables analysis of the microstructure uniformity of the cement-based composite. In general, a more uniform and dense microstructure (lower roughness value) should relate to a cement paste with higher mechanical properties and lower permeability. Before analysis, each image was plane fitted and flattened to eliminate image distortion from the microscope. Once image distortion was removed, the roughness values were calculated. Parts e and f of Figure 4 show the roughness analysis results of the regular cement paste and the nanomodified TiO_2 cement paste. As can be seen in these figures, the nanomodified TiO_2 cement paste has a much lower roughness value (92.851 nm), relative to that of the regular cement paste (406.60 nm), confirming pore refinement by nanomodification.

Figure 5 presents the AFM data of the height and phase images of the regular cement paste and cement paste modified with TiO_2 nanoparticles at 0.1 mass %, in a 10×10 μm^2 area. By a comparison of the height images of the two types of cement pastes (Figure 5a,b), it can be concluded that the incorporation of TiO_2 nanoparticles into the cement paste led to a flatter surface. Similarly, by comparing the phase images of the two types of cement pastes (Figure 5c,d), one can conclude that the phases of the paste modified with TiO_2 nanoparticles were much finer than those of the regular cement paste.

Assuming the general formula of C−S−H as $(CaO)_x(SiO_2)$-$(H_2O)_y$, the hydration reaction of normal Portland cement (C_3S/C_2S) can be simplified as

$$Ca_3SiO_5 + zCa_2SiO_4 + wH_2O \rightarrow (1 + z)(CaO)_x(SiO_2)(H_2O)_y + pCa(OH)_2 \quad (5)$$

In other words, because the total mole quantity of calcium is a constant, calcium can exist in the cement hydration products either as C−S−H gel or Portlandite in the hardened cement paste. As such, a lower amount of Portlandite corresponds to a higher amount of C−S−H gel. It is thus desirable to convert the noncementitious Portlandite into cementitious C−S−H gel. Any increase in the C−S−H amount or decrease in the Portlandite amount in concrete will lead to a higher performance of the hardened cement paste if the macrodefects in the concrete are ignored for such a comparison.

Figure 6 shows the XRD patterns of the ordinary Portland cement paste and the Portland cement paste modified with TiO_2 nanoparticles at 1.0 mass %, using Portlandite as the reference. It further confirms that the chemical reactions during the hydration process have been altered with the introduction of TiO_2 nanoparticles. As shown in Figure 6, the three main peaks characteristic of $Ca(OH)_2$ decreased by about 20−30% after the addition of TiO_2 nanoparticles, confirming the role of nanomodification in consuming Portlandite crystals. Such consumption of Portlandite likely led to a denser microstructure and the formation of desirable C−S−H gel, contributing to better engineering properties of the cement-based composite.

The direct reaction of $Ca(OH)_2$ and TiO_2 to form $CaTiO_3$ normally occurs only at high temperature over 1000 K. As such, no obvious $CaTiO_3$ peak was detected from the XRD data

dx.doi.org/10.1021/ie4011595 | Ind. Eng. Chem. Res. 2013, 52, 11575−11582

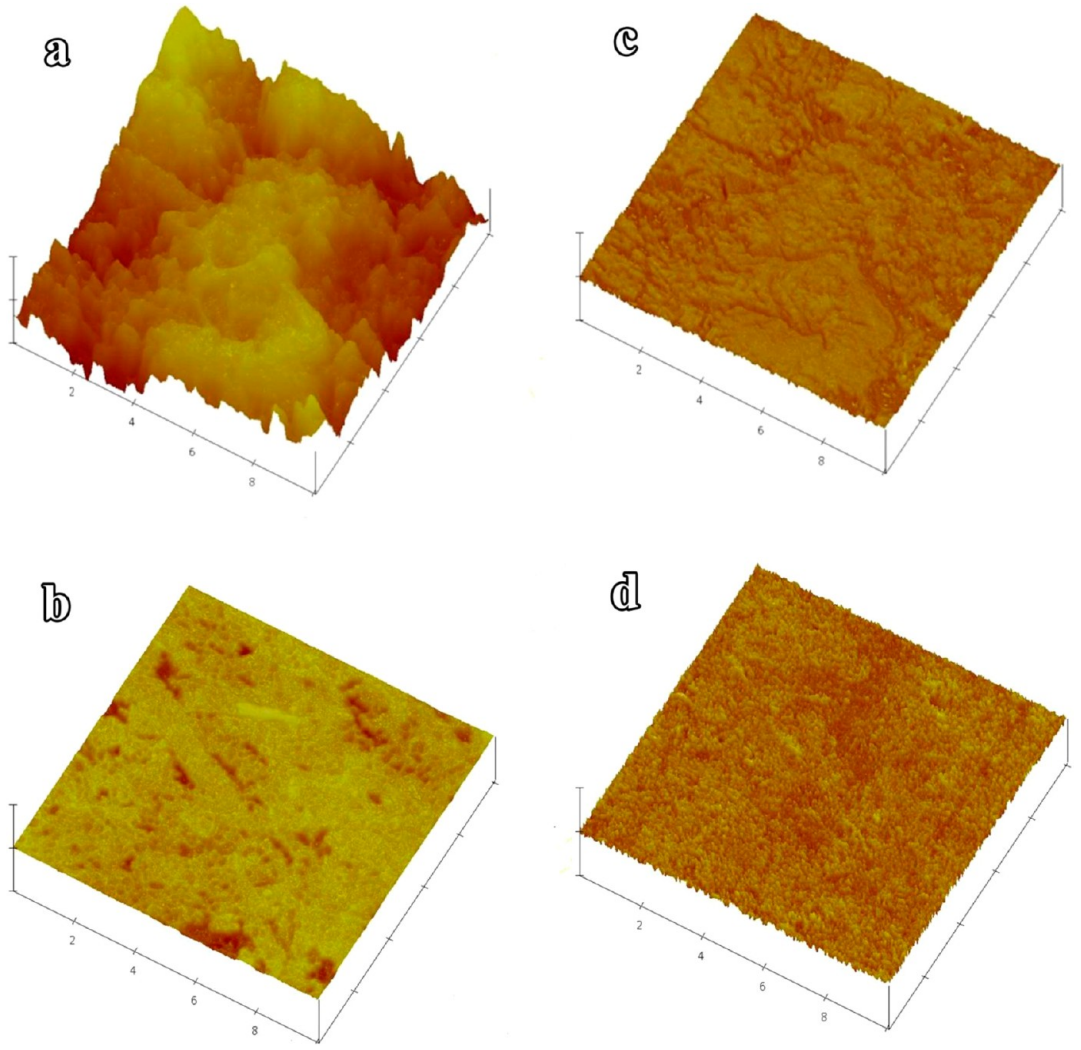

Figure 5. AFM observations of (a) height image of regular cement paste, (b) height image of cement paste modified by TiO_2 nanoparticles, (c) phase image of regular cement paste, and (d) phase image of cement paste modified by TiO_2 nanoparticles in a 10 × 10 μm^2 area.

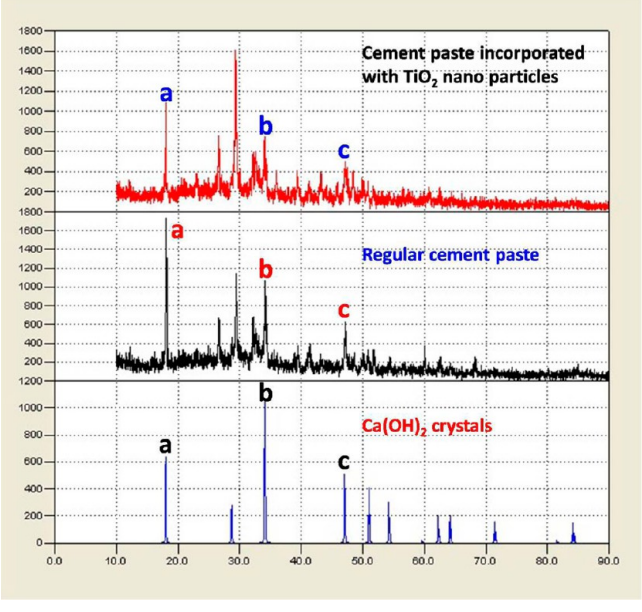

Figure 6. XRD patterns of the nanomodified TiO_2 Portland cement paste versus the regular Portland cement paste and Portlandite.

(Figure 6), suggesting the absence of crystallized $CaTiO_3$. During the cement hydration process, there is a possibility that the O^{2-} in −O−Ti−O− bonding is altered by hydroxyls (OH^-) to form the H−O−Ti−O−H structure. Subsequently, the H^+ in O−H can be replaced by Ca^{2+} to form the O−Ca− bond, which leads to the formation of the −Ca−O−Ti−O−Ca− structure. Because the quantity of the TiO_2 nanoparticles is relatively small, only a small fraction of the Ca^{2+} cations are consumed to form the nanosized −Ca−O−Ti−O−Ca− structure, which serves as a template around which the remaining Ca^{2+} cations react with Si^{4+} and OH^- to grow the needle-shaped amorphous hydration products.

4. CONCLUSIONS

The mechanical properties and microstructure of the cement pastes containing TiO_2 nanoparticles have been investigated through experimental research. The laboratory testing showed that the 28-day three-point bend strength of the cement paste with a water/cement ratio of 0.4 increased by 4.52%, 8.00%, 8.26%, and 6.71%, respectively, when 0.1%, 0.5%, 1.0%, and 1.5% TiO_2 nanoparticles by mass of cement were incorporated. Such improvements in the mechanical properties can be attributed to improvement of the paste microstructure. By the

dx.doi.org/10.1021/ie4011595 | Ind. Eng. Chem. Res. 2013, 52, 11575−11582

addition of a small amount (1.0 mass %) of TiO_2 nanoparticles and achievment of good dispersion, nanomodification increased the amount of cementitious phase in the paste, decreased the microporosity and amount of internal microcracks and defects, obtained a denser microstructure with reduced nanoroughness, and led to the formation of needle-shaped nanoprecipitates. The morphological information obtained at the micrometer and nanometer scales shed light on the role of TiO_2 nanoparticles in the cement-based composite. In summary, the admixing of TiO_2 nanoparticles into cement not only leads to denser hardened cement paste but also alters the morphology and chemical compositions of cement hydration products.

AUTHOR INFORMATION

Corresponding Author

*E-mail: xiening@hit.edu.cn (N.X.), xianming_s@coe.montana.edu (X.S.).

Notes

The authors declare no competing financial interest.

ACKNOWLEDGMENTS

This work was financially supported by the Natural Scientific Research Innovation Foundation in Harbin Institute of Technology (Grant HIT-NSRIF-2009100), The Lianyungang Scientific Plan-Industrial Program (Grant CG1204), The Jiangsu Province Ocean Resource Development Research Institute Science Open Fund Project (JSIMR11B10), and the China Postdoctoral Science Foundation (Grant 20110491065).

REFERENCES

(1) Richardson, I. G. The Calcium Silicate Hydrates. *Cem. Concr. Res.* **2008**, *38*, 137−158.

(2) Bullard, J. W.; et al. Mechanisms of cement hydration. *Cem. Concr. Res.* **2011**, *41*, 1208−1223.

(3) Jennings, H. M. Refinements to Colloid Model of C−S−H in Cement: CM-II. *Cem. Concr. Res.* **2008**, *38*, 275−289.

(4) Shi, X.; Fay, L.; Peterson, M. M.; Yang, Z. Freeze−Thaw Damage and Chemical Change of a Portland Cement Concrete in the Presence of Diluted Deicers. *Mater. Struct.* **2010**, *43*, 933−946.

(5) Rozière, E.; Loukili, A. R.; Hachem, E.; Grondin, F. Durability of Concrete Exposed to Leaching and External Sulphate Attacks. *Cem. Concr. Res.* **2009**, *39*, 1188−1198.

(6) Nehdi, M.; Pardhan, M.; Koshowski, S. Durability of Self-Consolidating Concrete Incorporating High-Volume Replacement Composite Cements. *Cem. Concr. Res.* **2004**, *34*, 2103−2112.

(7) Shi, X.; Xie, N.; Fortune, K.; Gong, J. Durability of Steel Reinforced Concrete in Chloride Environments: An Overview. *Constr. Build. Mater.* **2012**, *30*, 125−138.

(8) Bagheri, A. R.; Zanganeh, H.; Moalemi, M. M. Mechanical and Durability Properties of Ternary Concretes Containing Silica Fume and Low Reactivity Blast Furnace Slag. *Cem. Concr. Compos.* **2012**, *34*, 663−670.

(9) Pacheco-Torgal, F.; Ding, Y.; Jalali, S. Properties and durability of concrete containing polymeric wastes (tyre rubber and polyethylene terephthalate bottles): An overview. *Constr. Build. Mater.* **2012**, *30*, 714−724.

(10) Sanchez, F.; Sobolev, K. Nanotechnology in Concrete—A Review. *Constr. Build. Mater.* **2010**, *24*, 2060−2071.

(11) Birgisson, B.; et al. Nanotechnology in Concrete Materials—A Synopsis. *Transp. Res. Circ. E-C170* **2012**.

(12) Balaguru, P.; Chong, K. Nanotechnology and Concrete: Research Opportunities. *Proceedings of ACI Session on Nanotechnology of Concrete: Recent Developments and Future Perspectives*, Nov 7, 2006, Denver, CO.

(13) Birgisson, B.; Taylor, P.; Armaghani, J.; and Shah, S. P. American Roadmap for Research for Nanotechnology-Based Concrete Materials. *Transportation Research Record: Journal of the Transportation Research Board*, 2010; pp 130−138; No. 2142,

(14) He, X.; Shi, X. Chloride Permeability and Microstructure of Portland Cement Mortars Incorporating Nanomaterials. *Transportation Research Record: Journal of the Transportation Research Board*, 2008; pp 13−21; No. 2070.

(15) Zhang, M. H.; Li, H. Pore Structure and Chloride Permeability of Concrete Containing Nano-Particles for Pavement. *Constr. Build. Mater.* **2011**, *25*, 608−616.

(16) Li, H.; Xiao, H. G.; Yuan, J.; Ou, J. P. Microstructure of Cement Mortar with Nano-Particles. *Compos., Part B: Eng.* **2004**, *35*, 185−189.

(17) Shah, S. P.; Konsta-Gdoutos, M. S.; Metaxa, Z. S.; Mondal, P. Nanoscale Modification of Cementitious Materials. *Nanotechnol. Constr. 3* **2009**, 125−130.

(18) Li, Z.; Wang, H.; He, S.; Lu, Y.; Wang, M. Investigations on the Preparation and Mechanical Properties of the Nano-Alumina Reinforced Cement Composite. *Mater. Lett.* **2006**, *60*, 356−359.

(19) Makar, J. M.; Chan, G. W. Growth of Cement Hydration Products on Single-Walled Carbon Nanotubes. *J. Am. Ceram. Soc.* **2009**, *92*, 1303−1310.

(20) Vera-Agullo, J.; et al. Mortar and Concrete Reinforced with Nanomaterials. *Nanotechnol. Constr. 3* **2009**, 383−388.

(21) Kamat, P. V. TiO_2 Nanostructures. Recent Physical Chemistry Advances. *J. Phys. Chem. C* **2012**, *116*, 11849−11851.

(22) Dylla, H.et al. Evaluation of Environmental Effectiveness of Titanium Dioxide Photocatalyst Coating for Concrete Pavement. *Transportation Research Record: Journal of the Transportation Research Board*, 2010; pp 46−51; No. 2164.

(23) Hassan, M. M.; et al. Evaluation of the Durability of Titanium Dioxide Photocatalyst Coating for Concrete Pavement. *Constr. Build. Mater.* **2010**, *24*, 1456−1461.

(24) Shen, S.; Burton, M.; Jobson, B.; Haselbach, L. Pervious Concrete with Titanium Dioxide as a Photocatalyst Compound for a Greener Urban Road Environment. *Constr. Build. Mater.* **2012**, *35*, 874−883.

(25) Chang, T. P.; Shih, J. Y.; Yang, K. M.; Hsiao, T. C. Material Properties of Portland Cement Paste with Nanomontmorillonite. *J. Mater. Sci.* **2007**, *42*, 7478−7487.

(26) Mondal, P.; Shah, S. P.; Marks, L. A Reliable Technique to Determine the Local Mechanical Properties at the Nanoscale for Cementitious Materials. *Cem. Concr. Res.* **2007**, *37*, 1440−1444.

(27) Jo, B. W.; Kim, C. H.; Tae, G. H. Characteristics of Cement Mortar with Nano-SiO_2 Particles. *Constr. Build. Mater.* **2007**, *21*, 1351−1355.

(28) Jayapalan, A. R.; Lee, B. Y.; Kurtis, K. E. Effect of nano-sized titanium dioxide on early age hydration of Portland cement. *Nanotechnol. Constr. 3* **2009**, 267−273.

(29) Meng, T.; Yu, Y.; Qian, X.; Zhan, S.; Qian, K. Effect of nano-TiO_2 on the mechanical properties of cement mortar. *Constr. Build. Mater.* **2012**, *29*, 241−245.

(30) Lee, B. Y.; Kurtis, K. E. Influence of TiO_2 Nanoparticles on Early C_3S Hydration. *J. Am. Ceram. Soc.* **2010**, *93*, 3399−3405.

(31) Avrami, M. Kinetics of Phase Change 1—General Theory. *J. Chem. Phys.* **1939**, *7*, 1103−12.

(32) Avrami, M. Kinetics of Phase Change 2—Transformation-Time Relations for Random Distribution of Nuclei. *J. Chem. Phys.* **1940**, *8*, 212−24.

(33) Avrami, M. Granulation, Phase Change, and Microstructure-Kinetics of Phase Change III. *J. Chem. Phys.* **1941**, *9*, 177−84.

(34) Thomas, J. J. A New Approach to Modeling the Nucleation and Growth Kinetics of Tricalcium Silicate Hydration. *J. Am. Ceram. Soc.* **2007**, *90*, 3282−3288.

(35) Richardson, I. G. The Nature of C−S−H in Hardened Cements. *Cem. Concr. Res.* **1999**, *29*, 1131−1147.

(36) Allen, A. J.; Thomas, J. J.; Jennings, H. M. Composition and Density of Nanoscale Calcium−Silicate−Hydrate in Cement. *Nat. Mater.* **2007**, *6*, 311−316.

(37) Taylor, H. F. W. Proposed Structure for Calcium Silicate Hydrate Gel. *J. Am. Ceram. Soc.* **1986**, *69*, 464−467.
(38) Thomas, J. J.; Jennings, H. M.; Allen, A. J. Determination of the Neutron Scattering Contrast of Hydrated Portland Cement Paste Using H_2O/D_2O Exchange. *Adv. Cem.-Based Mater.* **1998**, *7*, 119−122.
(39) Bernal, J. D. The structure of cement hydration compounds. *Proc. 3rd Int. Symp. Chem. Cem., London* **1952**, 216−236.
(40) Ye, Q.; Zhang, Z. N.; Kong, D. Y. Influence of nano-SiO_2 addition on properties of hardened cement paste as compared with silica fume. *Constr. Build. Mater.* **2007**, *21*, 539−545.
(41) Han, B.; Yang, Z.; Shi, X.; Yu, X. Transport Properties of Carbon-Nanotube/Cement Composites. *J. Mater. Eng. Perform.* **2013**, *22*, 184−189.
(42) Li, H.; Zhang, M. H.; Ou, J. P. Flexural fatigue performance of concrete containing nano-particles for pavement. *Int. J. Fatigue* **2007**, *29*, 1292−1301.
(43) Edwards, C. L.; Alemany, L. B.; Barron, A. R. Solid-State Si-29 NMR Analysis of Cements: Comparing Different Methods of Relaxation Analysis for Determining Spin-Lattice Relaxation Times to Enable Determination of the C3S/C2S Ratio. *Ind. Eng. Chem. Res.* **2007**, *46*, 5122−5130.
(44) Haeussler, F.; Tritthart, J.; Amenitsch, H. Time-Resolved Combined SAXS and WAXS Studies on Hydrating Tricalcium Silicate and Cement. *Adv. Cem. Res.* **2009**, *21*, 101−111.
(45) Allen, A. J.; Thomas, J. J. Analysis of C−S−H Gel and Cement Paste by Small-Angle Neutron Scattering. *Cem. Concr. Res.* **2007**, *37*, 319−324.
(46) Skinner, L. B.; Chae, S. R.; Benmore, C. J.; Wenk, H. R.; Monteiro, P. J. M. Nanostructure of Calcium Silicate Hydrates in Cements. *Phys. Rev. Lett.* **2010**, *104*, 195502.
(47) Chen, J. J.; Sorelli, L.; Vandamme, M. A Coupled Nano-indentation/SEM-EDS Study on Low Water/Cement Ratio Portland Cement Paste: Evidence for C−S−H/Ca(OH)$_2$ Nanocomposites. *J. Am. Ceram. Soc.* **2010**, *93*, 1484−1493.
(48) Xu, Z.; Viehland, D. Observation of a Mesostructure in Calcium Silicate Hydrate Gels of Portland Cement. *Phys. Rev. Lett.* **1996**, *77*, 952−955.
(49) Sáez de Ibarra, Y.; Gaitero, J. J.; Erkizia, E.; Campillo, I. Atomic Force Microscopy and Nanoindentation of Cement Pastes with Nanotube Dispersions. *Phys. Status Solidi A* **2006**, *203*, 1076−1081.
(50) Wei, Y. Q.; Yao, W.; Xing, X. M.; Wu, M. J. Quantitative Evaluation of Hydrated Cement Modified by Silica Fume Using QXRD, ^{27}Al MAS NMR, TG-DSC and Selective Dissolution Techniques. *Constr. Build. Mater.* **2012**, *36*, 925−932.
(51) Scrivener, K. L.; Füllmann, T.; Gallucci, E.; Walenta, G.; Bermejo, E. Quantitative Study of Portland Cement Hydration by X-Ray Diffraction/Rietveld Analysis and Independent Methods. *Cem. Concr. Res.* **2004**, *34*, 1541−1547.
(52) Berra, M.; Carassiti, F.; Mangialardi, T. Effects of Nanosilica Addition on Workability and Compressive Strength of Portland Cement Pastes. *Constr. Build. Mater.* **2012**, *35*, 666−675.
(53) Anastasia, S.; Viktor, M.; Vyacheslav, K. Dispersion of Carbon Nanotubes and Its Influence on the Mechanical Properties of the Cement Matrix. *Cem. Concr. Compos.* **2012**, *34*, 1104−1113.
(54) Gavrila, R.; Dinescu, A.; Mardare, D. A Power Spectral Density Study of Thin Films Morphology Based on AFM Profiling. *Rom. J. Inf. Sci. Technol.* **2007**, *10*, 291−300.
(55) Kanda, T.; Li, V. C. Effect of Fiber Strength and Fiber-Matrix Interface on Crack Bridging in Cement Composites. *J. Eng. Mech.* **1999**, *125*, 290−299.
(56) Tucker, C. L., III; Liang, E. Stiffness Predictions for Unidirectional Short-fiber Composites: Review and Evaluation. *Compos. Sci. Technol.* **1999**, *59*, 655−671.